THE OXIDATION RATE OF SiC IN HIGH PRESSURE WATER VAPOR ENVIRONMENTS

e 420861

Elizabeth J. Opila
NASA Glenn Research Center/Cleveland State University
Department of Chemical Engineering
Cleveland, OH 44115

R. Craig Robinson
NASA Glenn Research Center/Dynacs Engineering Co.
Brookpark, OH 44142

CVD SiC and sintered α-SiC samples were exposed at 1316°C in a high pressure burner rig at total pressures of 5.7, 15, and 25 atm for times up to 100h. Variations in sample emittance for the first nine hours of exposure were used to determine the thickness of the silica scale as a function of time. After accounting for volatility of silica in water vapor, the parabolic rate constants for SiC in water vapor pressures of 0.7, 1.8 and 3.1 atm were determined. The dependence of the parabolic rate constant on the water vapor pressure yielded a power law exponent of one. Silica growth on SiC is therefore limited by transport of molecular water vapor through the silica scale.

INTRODUCTION

SiC is proposed for applications in high pressure, high temperature, and high gas velocity combustion environments such as turbine engines. Water vapor is always present in these environments as a product of combustion. Oxidation of SiC in water vapor occurs by the following reaction:

$$SiC + 3H_2O(g) = SiO_2 + CO(g) + 3H_2(g) \quad [1]$$

The rate of silica growth on SiC is described by the parabolic rate constant, k_p:

$$k_p = x^2/t \quad [2]$$

where x is the oxide thickness and t is time. Parabolic kinetics indicate that the growth of the silica scale is limited by transport through the growing silica scale. The effects of water vapor on SiC are known to be twofold. First, water vapor enhances the oxidation rate of SiC relative to the rates observed in dry oxygen (1). Second, water vapor reacts with the growing silica scale to form a volatile hydroxide as shown by the following reaction (2):

$$SiO_2 + 2H_2O(g) = Si(OH)_4(g) \qquad [3]$$

This reaction increases the recession rate of SiC (3). In order to predict the behavior of SiC in these environments, the kinetics of both reactions [1] and [3] must be understood as a function of pressure, temperature, and gas velocity.

This paper examines the dependence of the oxidation rate, k_p, on water vapor partial pressure, $P(H_2O)$. In the past, this effect has typically been examined at one atmosphere total pressure in furnace tests by varying the ratio of water vapor to a carrier gas, such as oxygen. This dependence can be described as:

$$k_p \propto P(H_2O)^n \qquad [4]$$

where n is the power law exponent. Results from previous studies are summarized in Table 1. Deal and Grove (4) found that the oxidation rate of silicon varied with the water vapor partial pressure independently of the carrier gas partial pressure for both argon and oxygen. Opila (1) suggested that the carrier gas, O_2 vs. Ar, may affect the measured oxidation rates of SiC in water vapor. In addition, bubbles found in the silica scale also affected the measured oxidation rates. The present study offers several advantages over previous studies. First, instead of varying the ratio of carrier gas to water vapor at one atmosphere pressure, the gas composition is kept constant and the total pressure is varied. This eliminates effects of variations in carrier gas partial pressures. Secondly, the oxidation rate measurements in this study were only possible at short times when the silica film was amorphous and homogeneous. The technique does not work for silica scales which are rough (crystalline or bubbled scales.) Thus, by the nature of the technique, crystallization and bubbling effects are eliminated.

Table 1. Literature values for the dependence of k_p on the water vapor partial pressure: $k_p \propto P(H_2O)^n$.

Study	Material	Carrier gas	n	Temperature (°C)
Deal & Grove (4)	Si	O_2, Ar	1	1000-1200
Opila (1)	SiC	O_2	0.85,0.76	1200, 1400
Opila (1)	SiC	Ar	0.67	1100
Antill & Warburton (5)	Si	none?	0.67	1000, 1200

Determination of the value of the power law exponent, n, shown in Equation 4 allows the identification of the rate limiting oxidant species. Since the parabolic rate constant is proportional to the concentration of the rate limiting diffusing defect species, the parabolic rate constant will have the same water vapor partial pressure dependence as the oxidant defect species as determined from the defect formation reaction (6). For example, given silica growth limited by molecular water vapor diffusion through the silica scale, the power law exponent will have a value of one. The derivation of the power law exponents for several water vapor defect species are shown in detail in Table 2.

Table 2. Water vapor partial pressure dependence for several water vapor defect species using standard Kroger-Vink notation.

Water vapor defect species	Defect formation reaction	Mass action expression	Electro-neutrality expression	Water vapor partial pressure dependence	Power law exponent, n
$H_2O^x_i$	$H_2O(g) = H_2O^x_i$	$K_1=[H_2O^x_i]/P_{H2O}$	none	$[H_2O^x_i] \propto P_{H2O}^{1}$	1
OH'_i	$H_2O(g)=OH'_i+H^{\bullet}_i$	$K_2=[OH'_i][H^{\bullet}_i]/P_{H2O}$	$[OH'_i]=[H^{\bullet}_i]$	$[OH'_i] \propto P_{H2O}^{1/2}$	1/2

The objectives of this work are to determine the parabolic rate constants of SiC in water vapor, to determined the dependence of the oxidation rate constant on the water vapor pressure, and finally to use this dependence to determine the mechanism of SiC oxidation in water vapor.

EXPERIMENTAL PROCEDURE

The material used in this study was high purity chemical vapor deposited (CVD) silicon carbide (SiC) or sintered α-SiC (Carborundum) coupons of dimensions 2.54 x 1.27 x 0.32 cm (1 x 1/2 x 1/8 inch). These coupons were exposed in a high pressure

burner rig (HPBR) at 1316°C (2400°F) at an equivalence ratio of 0.9. The gas pressures, velocities, and chemistry can be found in Table 3. Samples were exposed up to 100h, however, for the purposes of this study, results from only the first nine hours were used. Sample temperature was monitored with a two color pyrometer.

Table 3. HPBR test conditions.

Test condition	Total pressure, atm	Gas velocity, m/s	Gas composition
1	5.7	20	12.3% H_2O, 2.1% O_2
2	15	10	11.0% CO_2, 71.8% N_2
3	25	5	

RESULTS AND DISCUSSION

Upon exposure of SiC samples in the HPBR, the apparent temperature of the sample, as measured by the pyrometer, fluctuated in a systematic manner as shown in Figure 1. This fluctuation was attributed to variations in sample emittance as the silica scale grew, as previously described by Schiroky (7). A schematic diagram of the emittance of a SiC substrate covered with a transparent silica film is shown in Figure 2. The amplitude of the emitted wave is the sum of the individual emitted waves. For some silica thickness, d_{max}, given by

$$d_{max} = [(2m+1)\pi - \beta]\, \lambda/4\pi n \qquad [5]$$

there is constructive interference of the waves so that the apparent temperature as monitored by the pyrometer reaches a maximum. Here m is zero or a positive integer value, β is the phase shift which occurs at the silica/silicon carbide interface, λ is the wavelength monitored by the pyrometer, and n is the refractive index of silica. Values used in these calculations are shown in Table 4. Details of the derivation and calculation of the scale thickness can be found in Reference (7). As the scale continues to grow the interference between the emitted waves becomes destructive and a minimum in the apparent temperature is observed at a scale thickness of d_{min} given by:

$$d_{min} = [2m\pi - \beta]\, \lambda/4\pi n \qquad [6]$$

The apparent temperature, as measured by the pyrometer, continues to fluctuate through maxima and minima as the scale grows until the optical properties of the scale are

degraded by crystallization or surface roughness. In this study, the maximum time at which extrema in the apparent temperature were measured was nine hours. The time at which each peak occurs corresponds to the scale thickness as determined from Equations 5 and 6 as shown in Figure 1. The scale thickness was then plotted versus time as shown in Figure 3.

Table 4. Values used to calculate silica thickness from Equations 5 and 6. k is the absorption coefficient.

$\beta = 2n_2k_3/(n_3^2 - n_2^2 + k_3^2)$	0.14π
λ	1.0 μm
$n_2 = n(SiO_2)$	1.5
$n_3 = n(SiC)$	2.7
$k_3 = k(SiC)$	1.0

The rate constants for oxidation can then be determined from the oxide growth kinetics shown in Figure 3. As previously mentioned, the oxide thickness on SiC in the HPBR is determined by both the rate of silica growth, k_p, and the rate of silica volatilization, k_l. Tedmon has derived an expression for the paralinear oxide growth of chromia scales (8). This expression is directly applicable to SiC oxidation in water vapor:

$$t = \frac{k_p}{2k_l^2}\left[-\frac{2k_l x}{k_p} - \ln\left(1 - \frac{2k_l x}{k_p}\right)\right] \tag{7}$$

Since x and t are known, and k_p is to be determined, the values of k_l are needed first. In fact, k_l has been determined experimentally in the HPBR over a range of conditions and has been calculated for the conditions of this study using the following expression (3):

$$k_l = 2.04\,\rho\left[e^{-108kH/\text{mole}RT}\right]P^{1.50}\,v^{0.50} \tag{8}$$

Here ρ is the density of SiC, 3.1 g/cm^3, T is the temperature in K, P is the pressure in atm, and v is the gas velocity in m/s. The values of k_p and k_l for each test, determined from Equations 7 and 8 respectively, are shown in Table 5. The fit of the oxide thickness vs. time data to the Tedmon Equation (Equation 7) is shown as the solid lines in Figure 3. The mechanism of silica volatility for SiC in water vapor has been examined in detail

already (3,9). It is the intent of this paper to examine the oxidation mechanism described by the parabolic rate constant.

Table 5. Rate constants for SiC oxidation and volatilization in the HPBR at 1316°C.

total pressure, (atm)	water vapor partial pressure, (atm)	gas velocity, (m/s)	k_l, (μm/h)	k_p, (μm^2/h)
5.7	0.70	20	0.109	0.28, 0.31, 0.31
15	1.85	10	0.331	0.68, 0.65
25	3.09	5	0.490	1.20, (1.40)

Before examining the results for k_p as a function of water vapor partial pressure a brief discussion of the mixed oxidants present in the combustion environment is warranted. It is assumed here that the oxidation rate described by k_p is dependent only the water vapor partial pressure and the oxidation due to oxygen and carbon dioxide is negligible. This assumption seems reasonable based on the following discussion. The oxidation rate of SiC in one atm dry oxygen at 1300°C is $4x10^{-2}$ μm^2/h (10). The oxygen partial pressures in the present study ranged from 0.12 to 0.52 atm. Therefore, the parabolic oxidation rate due to oxygen alone in the present study should be less than $2x10^{-2}$ μm^2/h. Values of k_p for SiC in the combustion gas mixture (Table 5) vary between $2.8x10^{-1}$ to 1.4 μm^2/h. Contributions of oxygen to the overall oxidation rate are less than 7%. In addition, it has been shown that oxidation in carbon dioxide is negligible even compared to oxygen (11).

The dependence of the parabolic oxidation rate on the water vapor partial pressure is shown in Figure 4. It can be seen that the power law exponent has a value of 0.97±0.15 (95% confidence) which is not statistically different from one. By comparison with the information in Table 2, the rate of oxide growth on SiC in water vapor is limited by transport of molecular water vapor through the silica scale. This differs with previous results (1,5), but here ambiguities related to carrier gases, crystallization, and bubbles in the silica scale are not present.

SUMMARY AND CONCLUSIONS

The oxidation rates of CVD SiC and sintered α-SiC have been determined in a high pressure burner rig at 1316°C and water vapor partial pressures of 0.7, 1.8, and 3.1 atm. After accounting for silica volatilization, the parabolic oxidation rate for SiC was found to vary with water vapor partial pressure with a power law exponent of 0.97±0.15. This result indicates that oxide growth on SiC in water vapor is limited by transport of molecular water vapor through the silica scale.

ACKNOWLEDGMENTS

The authors would like to acknowledge Bob Miller and Carl Stearns (retired) of NASA Glenn Research Center for recognizing that the fluctuations in the apparent measured temperature could be used to determine oxide thickness.

REFERENCES

1. E. J. Opila, J. Am. Ceram. Soc., **82**, 625 (1999).
2. E. J. Opila and R. E. Hann, Jr., J. Am. Ceram. Soc., **80**, 197 (1997).
3. R. C. Robinson and J. L. Smialek, J. Am. Ceram. Soc., **82**, 1817 (1999).
4. B. E. Deal and A. S. Grove, J. Appl. Phys., **36**, 3770 (1965).
5. J. E. Antill and J. B. Warburton, in Reactions Between Solids and Gases, p. 10-1, AGARD CP-52, Advisory Group for Aerospace Research and Development, Paris, France (1970).
6. P. Kofstad, High Temperature Corrosion, p. 72, Elsevier Applied Science Publishers Ltd., New York (1988).
7. G. H. Schiroky, J. Mat. Sci., **22**, 3595 (1987).
8. C. S. Tedmon, Jr., J. Electrochem. Soc., **113**, 766 (1967).
9. E. J. Opila, J. L. Smialek, R. C. Robinson, D. S. Fox, N. S. Jacobson, J. Am. Ceram. Soc., **82**, 1826 (1999).
10. L. U. J. T. Ogbuji and E. J. Opila, J. Electrochem. Soc., **142**, 925 (1995).
11. E. J. Opila and Q. N. Nguyen, J. Am. Ceram. Soc., **81**, 1949 (1998).

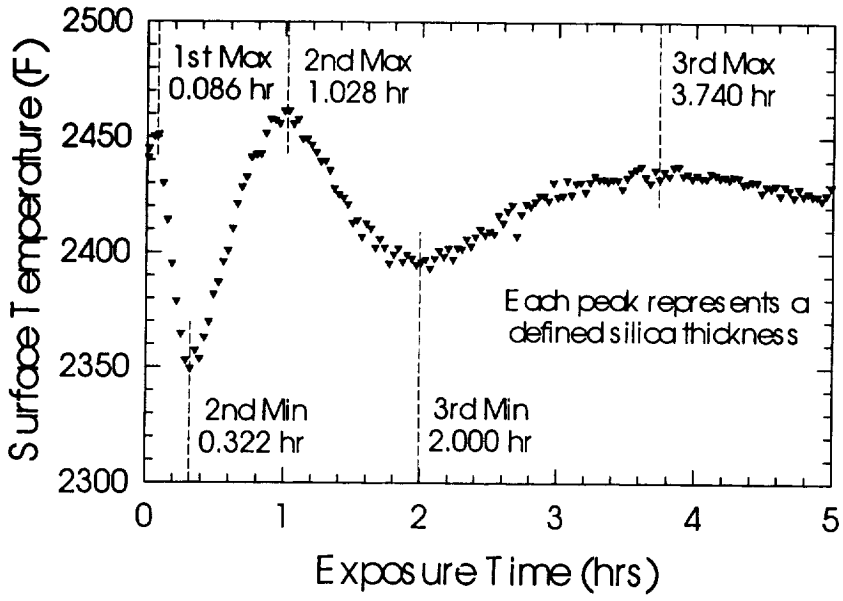

Figure 1. Variation of apparent temperature of SiC with oxide thickness and time.

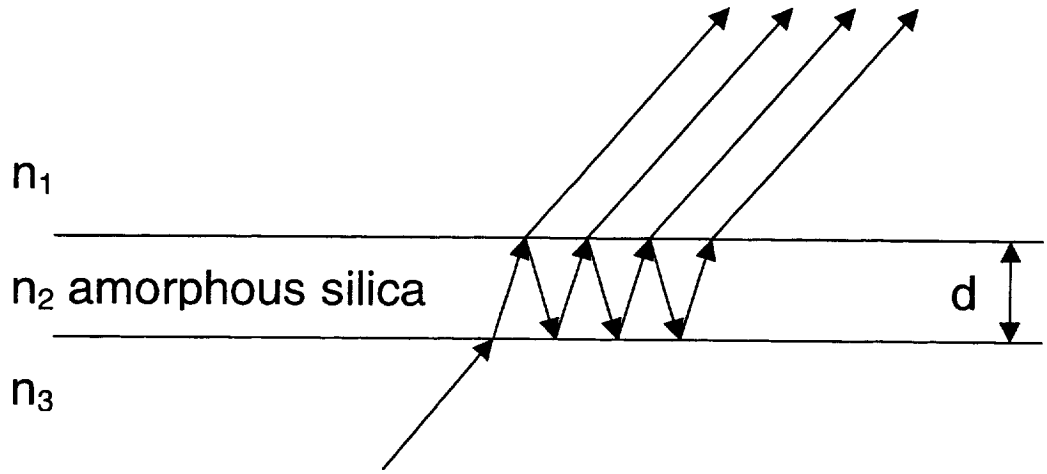

Figure 2. Schematic drawing of emittance of a SiC substrate with a transparent amorphous silica scale.

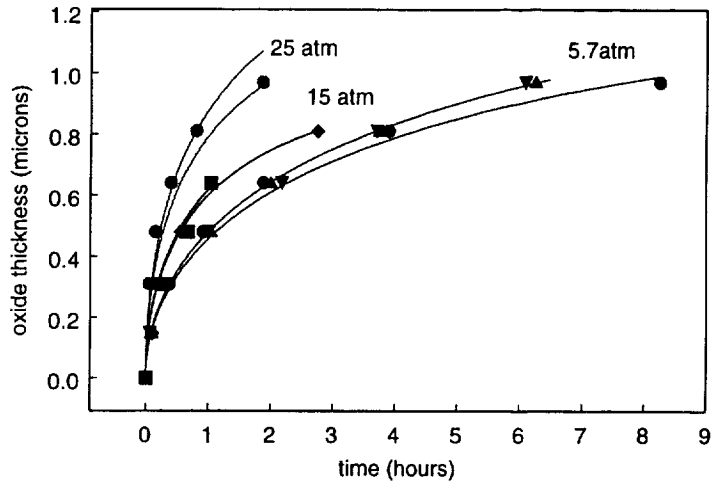

Figure 3. Variation of oxide scale thickness on SiC as a function of total pressure and time. Symbols represent thicknesses determined from Equations 5 and 6. Solid lines represent best fit to the Tedmon Equation (Equation 7).

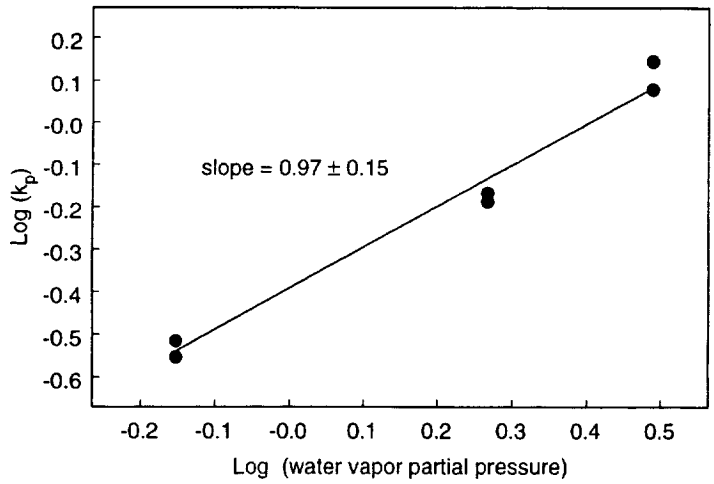

Figure 4. Variation of SiC oxidation rate with water vapor partial pressure.